Meta learning-based open-set identification system for specific emitter identification in non-cooperative scenarios

Cunxiang Xie[1], Limin Zhang[1], and Zhaogen Zhong[1*]
[1] Naval Aviation University
Yantai 264001, China
[E-mail : 15953599208@163.com]
[*]Corresponding author: Zhaogen Zhong

Received March 30, 2022; revised May 10, 2022; accepted May 12, 2022; published May 31, 2022

Abstract

The development of wireless communication technology has led to the underutilization of radio spectra. To address this limitation, an intelligent cognitive radio network was developed. Specific emitter identification (SEI) is a key technology in this network. However, in realistic non-cooperative scenarios, the system may detect signal classes beyond those in the training database, and only a few labeled signal samples are available for network training, both of which deteriorate identification performance. To overcome these challenges, a meta-learning-based open-set identification system is proposed for SEI. First, the received signals were pre-processed using bi-spectral analysis and a Radon transform to obtain signal representation vectors, which were then fed into an open-set SEI network. This network consisted of a deep feature extractor and an intrinsic feature memorizer that can detect signals of unknown classes and classify signals of different known classes. The training loss functions and the procedures of the open-set SEI network were then designed for parameter optimization. Considering the few-shot problems of open-set SEI, meta-training loss functions and meta-training procedures that require only a few labeled signal samples were further developed for open-set SEI network training. The experimental results demonstrate that this approach outperforms other state-of-the-art SEI methods in open-set scenarios. In addition, excellent open-set SEI performance was achieved using at least 50 training signal samples, and effective operation in low signal-to-noise ratio (SNR) environments was demonstrated.

Keywords: Cognitive radio; Specific emitter identification; Open-set identification system; Meta learning.

1. Introduction

The development of wireless communication technology has led to an increase in the demand for spectrum resources [1, 2]. In sharp contrast, most allocated spectrum resources are not fully utilized, which is in contraction to the purported lack of spectrum resources and the low utilization of licensed frequency bands [3]. In traditional wireless communication, a wireless spectrum is statically allocated. As such, licensed users or primary users (PUs) always occupy a fixed frequency band. Regardless of whether the frequency band is used, unlicensed or secondary users (SUs) cannot occupy it [4]. This ensures communication quality, but is an inefficient use of spectrum resources that results in low spectrum utilization. To solve this spectrum under-utilization problem, a cognitive radio (CR) network has been proposed [5-7]. In this network, the spectrum is monitored to establish the presence of PUs. Spectrum monitoring [8, 9] facilitates the detection of spectrum holes, which can be used by SUs when they are not used by PUs, thereby improving spectrum utilization. During operation, the radio frequency (RF) signal status of the PUs is monitored to ensure that SUs can quickly exit a spectrum when it is accessed by PUs.

However, it is necessary to monitor whether PUs operate within the allocated spectrum resources and to detect when SUs access the normal communication spectrum. The realization of spectrum monitoring and management to determine the working status of PUs and SUs requires the application of specific emitter identification (SEI) technology, which is used to identify individual emitters based on the subtle characteristics extracted from RF signals [10-13]. These characteristics define regular tendencies that repeat in all the RF signals transmitted by an emitter device, which are generated from the imperfection of the emitter hardware and are unique to each emitter. Therefore, the characteristics are also known as RF fingerprints (RFFs) [14, 15].

SEI has been extensively studied in recent years. Padilla et al. [16] proposed a method for extracting RFFs based on the spectral information of communication preambles, which successfully identified multiple Wi-Fi devices. In the study presented in [17], a Hilbert-Huang transform was applied to the transient RF signals generated by eight individual emitters to obtain the Hilbert-Huang transform-based time-frequency-energy distribution of the signals, and 13 time-frequency characteristic parameters were designed and extracted as RFFs to perform SEI. Satija et al. [18] proposed a variational mode decomposition algorithm to decompose RF signals to obtain spectral mode components, then performed a Hilbert-Huang transform on the spectral mode components to extract various spectral features including spectral flatness, spectral brightness, and spectral roll-off, which were then used as RFFs for SEI tasks. Zhou et al. [19] reported on an SEI method based on the bispectrum-radon transform. In this approach, the bi-spectral energy distribution of the received RF signals was initially obtained via bi-spectral analysis. This was followed by feature compression using the Radon transform to reduce computational complexity. The hybrid deep model was used to process compressed feature vectors to further extract deep features and complete the SEI task.

RFFs are generated by the interaction of different nonlinear operating elements within an emitter, which are difficult to model accurately and completely using mathematical models. However, conventional, manual and predefined feature extraction methods are only effective for specific types of signals, and it is difficult to completely and deeply extract RFFs from emitter signals with complex features. The latest advances in artificial intelligence (AI) [20, 21] has resulted in the application of deep learning [22, 23] techniques to modulation classification [24, 25] and radio signal recognition [26, 27]. Furthermore, various deep learning-based approaches have been developed for SEI. The powerful fitting ability of neural

networks facilitates the comprehensive and adaptive extraction of RFFs, which represents a new research direction. Ding et al. [28] processed the integrated bispectrum of an emitter signal using a convolutional neural network (CNN). Subsequently, they extracted the overall feature information that was hidden in the original signal. The experimental results demonstrate the superiority of this method compared to traditional fingerprint feature extraction techniques. To overcome the problem of the partial loss of signal characteristics caused by the integral bispectrum, Pan et al. [29] used a residual neural network to process the grayscale image of the spectrum obtained when the Hilbert–Huang transform of a signal was performed. Their experimental results demonstrate the superiority of the classification performance of this approach. Recurrence plot (RP) transform, continuous wavelet transform, and short-time Fourier transform have been investigated [30] in relation to RF signals. In this investigation, the amplitude of the transformed data was used as the input to a CNN, which successfully distinguished 12 wireless communication devices. Wong et al. [31] used a CNN to estimate the gain and phase deviations of the in-phase and quadrature components of an emitter signal, and achieved SEI based on the estimated gain deviation and phase deviation. This method does not require pre-processing, such as signal synchronization and carrier frequency tracking, and can be applied to signals of multiple modulation types. Liu et al. [32] proposed a network model for SEI that consisted of a deep bidirectional long short-term memory (Bi-LSTM) network and a one-dimensional residual CNN. This network model performed dilated convolution and generated squeeze-and-excitation blocks for extracting the hidden RFF features in baseband signals, in addition to SEI. The simulation results revealed that this method can effectively identify 16 USRP devices or five Zigbee devices. Wang et al. [33] reported on a novel deep-learning (DL)-based model of a complex-valued neural network (CVNN) for the direct processing of complex basebands and RF signals. Therefore, the CVNN can perform SEI more adaptively and effectively. This method can achieve almost 100% identification accuracy at a signal-to-noise ratio (SNR) of 25 dB, and the designed network can converge within 50 training epochs, which is indicative of excellent identification and convergence performance. Qian et al. [34] proposed an automatic SEI system based on a CNN with multilevel sparse representation identification (MSRI). The SEI system spliced the shallow and deep RFF features extracted by the CNN, then performed SEI based on sparse representation. Using at least 15 training samples, this method can identify nine emitter devices with an identification accuracy above 90%.

Previous DL-based studies have focused on closed-set SEI wherein the RF signals to be identified are all from known classes i.e., the RF signal classes in the training dataset include the RF signal classes in the test dataset. However, SEI technology is mainly applied to non-cooperative scenarios. Thus, the closed-set assumption used in these methods may be violated because of the presence of RF signals from unknown classes. In this case, traditional identification systems that observe RF signals from unknown classes are forced to identify them as one of the known classes, which deteriorates the identification performance of SEI systems. The detection of RF signals from unknown classes while classifying known classes of RF signals, also known as open-set SEI, has not been reported in the literature to date. Furthermore, only a few labeled signal samples can be obtained and used for training in non-cooperative scenarios. Therefore, the investigation of a solution to the few-shot problem of an open-set SEI has practical merit. In this study, we propose a meta-learning-based open-set identification system for SEI in non-cooperative scenarios. The main contributions of this study can be summarized as follows:

1) We propose an RF signal pre-processing method based on bi-spectral analysis and Radon transform to obtain signal representation vectors that can characterize RFFs for RF

signals, which lays the foundation for subsequent neural network processing.

2) An open-set SEI network is proposed, which consists of a deep feature extractor and an intrinsic feature memorizer. The training loss function of the open-set SEI network is then designed, which consists of a classification loss function and a detection loss function that can simultaneously optimize the parameters of both the deep feature extractor and intrinsic feature memorizer. The trained open-set SEI matches the intrinsic feature memorizer parameters with the output of the deep feature extractor, thereby detecting unknown classes and classifying different known classes.

3) To solve the few-shot problem of the open-set SEI, we designed the meta-training loss function and procedure based on the original open-set SEI network, simultaneously optimizing the parameters of both the deep feature extractor and intrinsic feature memorizer using only a few labeled samples and achieving excellent open-set SEI performance.

4) Numerous experiments were performed to evaluate the open-set identification performance of the proposed method. First, we evaluated our method using varying degrees of openness. Compared with state-of-the-art techniques, our method was superior in terms of the open-set SEI. We also evaluated the influence of the number of training samples on the open-set SEI performance, and the results showed that the proposed approach performed well using a limited number of training samples. Finally, we evaluated the performance of the technique for different SNRs, which revealed strong noise robustness.

The remainder of this paper is organized into different sections. Section 2 introduces the signal pre-processing method, Section 3 presents the details of the meta-learning-based open-set SEI network, Section 4 reviews and discusses the experimental results, and Section 5 summarizes the main findings of this study.

2. Signal Pre-processing

2.1 Bi-spectral analysis

Bi-spectral analysis, which is best suited for dealing with non-Gaussian and non-smooth signals, is essentially a two-dimensional Fourier transform of the third-order cumulants of a signal [35]:

$$\begin{aligned} B(\omega_1,\omega_2) &= \sum_{\tau_1}\sum_{\tau_2} C_{3x}(\tau_1,\tau_2) e^{-j(\omega_1\tau_1+\omega_2\tau_2)} \\ &= \sum_{\tau_1}\sum_{\tau_2} E\left[x(t)x(t+\tau_1)x(t+\tau_2)\right] e^{-j(\omega_1\tau_1+\omega_2\tau_2)} \end{aligned} \tag{1}$$

where ω_1, ω_2 denote the two-dimensional frequencies.

2.1.1 Radon transform

A bi-spectral distribution can effectively characterize the RFFs of RF signals. However, this introduces a high computational burden when a two-dimensional bi-spectral distribution is directly used for subsequent neural network processing. Therefore, we introduce a Radon transform to project a two-dimensional bi-spectral distribution onto a one-dimensional projection feature vector, which is defined as a signal representation vector.

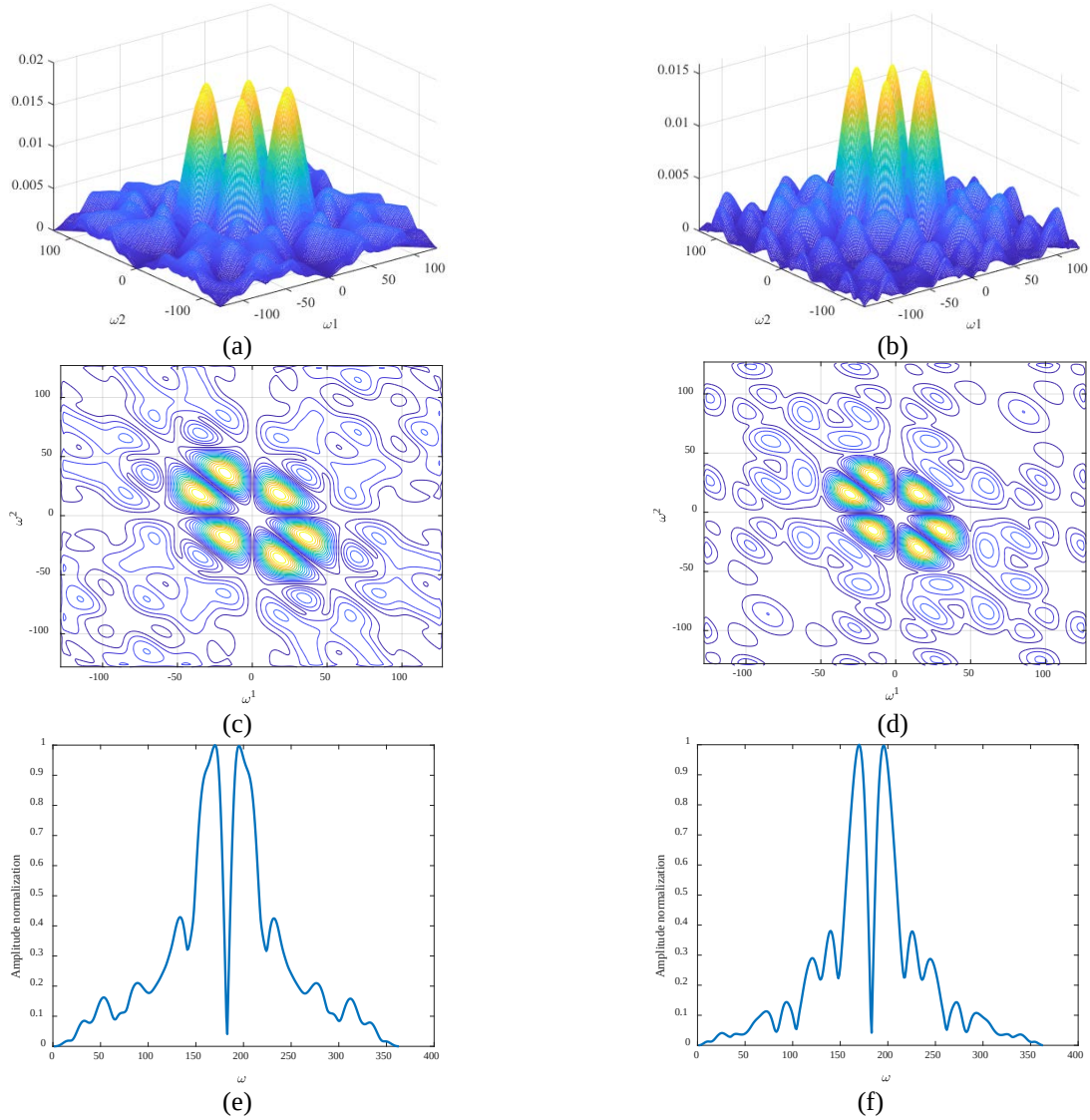

Fig. 1. Bi-spectral distribution and one-dimensional projected feature map of RF signals: (a) Three-dimensional bi-spectral energy distribution of $x_1(t)$. (b) Three-dimensional bi-spectral energy distribution of $x_2(t)$. (c) Two-dimensional bi-spectral distribution of $x_1(t)$. (d) Two-dimensional bi-spectral distribution $x_2(t)$. (e) One-dimensional projection feature map of $x_1(t)$. (f) One-dimensional projection feature map of $x_2(t)$.

The Radon transform [36, 37] calculates the linear integral of a two-dimensional function over any line in a two-dimensional plane xOy. For bi-spectral distribution $B(\omega_1, \omega_2)$, the Radon transform can be expressed as follows:

$$R(\theta,\rho)=\int_{-\infty}^{\infty}\int_{-\infty}^{\infty}B(\omega_1,\omega_2)\delta(\rho-\omega_1\cos\theta-\omega_2\sin\theta)d\omega_1 d\omega_2 \tag{2}$$

where θ is the angle between the target line and the coordinate axis, and ρ is the perpendicular distance of the target line from the origin. The characteristic function δ is defined as follows.

$$\delta(x)=\begin{cases}0 & x\neq 0\\ 1 & x=0\end{cases} \tag{3}$$

The characteristic function is used to ensure that the integration proceeds along the line $\rho=\omega_1\cos\theta+\omega_2\sin\theta$.

Fig. 1 illustrates the bi-spectral distribution of the RF signals $x_1(t)$, and $x_2(t)$ that are collected from two emitter and their one-dimensional projected feature maps obtained using the Radon transform. In the Radon transform, we let $\rho=0$ and $\theta=3\pi/4$ i.e., we take the linear integral over the straight line $\omega_1=\omega_2$ and normalize the integration result.

As shown in **Fig. 1**, there are visible differences between different three-dimensional bi-spectral energy distributions, two-dimensional bi-spectral distributions, and one-dimensional projection feature maps, which suggest that bi-spectral analysis can intuitively and effectively highlight RFFs for RF signals collected from different emitters.

3. Proposed Method

3.1 Open-set SEI Network

The traditional closed-set SEI network consists of two main components: (1) the deep feature extractor that maps the signal representation vector $\boldsymbol{x}$ into the penultimate layer output $f_\theta(\boldsymbol{x})$, where θ represents deep feature extractor parameters; and (2) a SoftMax classifier [38, 39] $C\left(f_\theta(\boldsymbol{x});\boldsymbol{w}_k\right)$, which estimates signal class posterior probabilities based on the penultimate layer output $f_\theta(\boldsymbol{x})$:

$$p(y\mid\boldsymbol{x};\theta,\boldsymbol{w}_k)=\frac{\exp\left(\boldsymbol{w}_y^T f_\theta(\boldsymbol{x})\right)}{\sum_{y'}\exp\left(\boldsymbol{w}_{y'}^T f_\theta(\boldsymbol{x})\right)} \tag{4}$$

where $\boldsymbol{w}_k$ represents the SoftMax classifier parameters, and y represents the class label corresponding to $\boldsymbol{x}$. Furthermore, a metric-learning-based SoftMax classifier is proposed to simplify the network structure.

$$p(y\mid\boldsymbol{x};\theta)=\frac{\exp\left\{-\left\|f_\theta(\boldsymbol{x})-E\left[f_\theta(\boldsymbol{x})\mid y\right]\right\|_2^2\right\}}{\sum_{y'}\exp\left\{-\left\|f_\theta(\boldsymbol{x})-E\left[f_\theta(\boldsymbol{x})\mid y\right]\right\|_2^2\right\}} \tag{5}$$

However, the SoftMax classifier only estimates posterior probabilities for known signal classes and limits their sum to one, i.e., $\sum_y p(y\mid\boldsymbol{x})=1$. Therefore, it is only applied to a closed-set SEI, which assumes that the testing signal classes $\mathbb{C}^t$ are identical to the training signal classes $\mathbb{C}^s$. However, in realistic scenarios, some testing signal classes $\mathbb{C}^u$ are not present in the training signal classes $\mathbb{C}^s$, i.e., $\mathbb{C}^t=\mathbb{C}^s\cup\mathbb{C}^u$ [40-42]. In this case, unknown signal classes are regarded as known signal classes and assigned an inappropriately high probability, causing signal samples of unknown classes to be misclassified as one of the known

classes, as shown in **Fig. 2(a)**. Therefore, the detection of unknown signal classes during the classification of known signal classes is a common problem that should be studied.

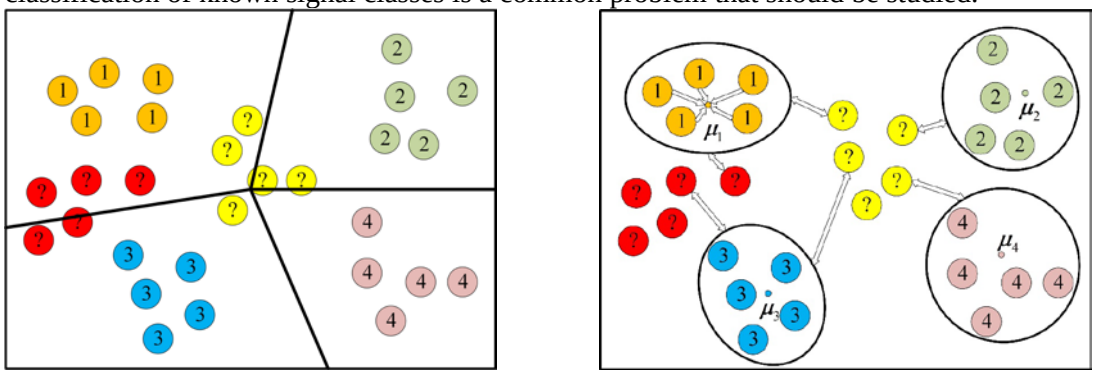

Fig. 2. Signal deep features $f_\theta(\boldsymbol{x})$ of 4 known classes and 2 unknown classes in feature space: (a) based on traditional SoftMax classifier, signals of unknown classes are misclassified as one of the known classes, (b) intrinsic feature memorizer parameters of 4 known classes can be denoted as $\boldsymbol{\mu}_1, \boldsymbol{\mu}_2, \boldsymbol{\mu}_3, \boldsymbol{\mu}_4$, and signal deep features $f_\theta(\boldsymbol{x})$ of each class j, clustered around $\boldsymbol{\mu}_j$, and far away from other known classes $\boldsymbol{\mu}_l (l \neq j)$ and unknown classes.

Inspired by the metric-learning-based SoftMax classifier, we propose an open-set SEI network, which abandons the SoftMax classifier and replaces it with the intrinsic feature memorizer, and introduces the new parameters of $\{\boldsymbol{\mu}_j \mid j \in \{1,2,\cdots,C\}\}$, referred to as intrinsic feature memorizer parameters. The intrinsic feature memorizer parameters contain C vectors, with the same dimension as the penultimate layer output vectors, corresponding to C known signal classes. Parameters $\{\boldsymbol{\mu}_j\}$ can be optimized via network training, and the optimized $\{\boldsymbol{\mu}_j\}$ can memorize the intrinsic features of the received RF signals, which are class-unique. The open-set SEI network can match the parameters $\{\boldsymbol{\mu}_j\}$ with the signal deep features $f_\theta(\boldsymbol{x})$ extracted using the deep feature extractor. this facilitates the detection of unknown classes and the classification of different known classes, as shown in **Fig. 2(b)**.

In the open-set SEI network training process, both the deep feature extractor parameters θ and the intrinsic feature memorizer parameters $\{\boldsymbol{\mu}_j\}$ were optimized based on the training signal dataset. The key to parameter optimization is in the design of the training loss function, which consists of two parts: a classification loss (*CL*) function and a detection loss (*DL*) function.

For the *CL* function, we first calculate the probability that a signal deep feature sample $f_\theta(\boldsymbol{x})$ matches its corresponding intrinsic feature memorizer parameters $\boldsymbol{\mu}_y$:

$$p(y \mid \boldsymbol{x}) = p(\boldsymbol{\mu}_y \mid \boldsymbol{x}) = \frac{\exp\left(-\left\| f_\theta(\boldsymbol{x}) - \boldsymbol{\mu}_y \right\|_2^2\right)}{\sum_{k=1}^{C} \exp\left(-\left\| f_\theta(\boldsymbol{x}) - \boldsymbol{\mu}_k \right\|_2^2\right)} \tag{6}$$

We then calculate the probability that the same signal deep feature sample $f_\theta(\boldsymbol{x})$ matches with the intrinsic feature memorizer parameters $\boldsymbol{\mu}_c(c \neq y)$ that belong to other known signal classes:

$$p(c \mid \boldsymbol{x}) = p(\boldsymbol{\mu}_c \mid \boldsymbol{x}) = \frac{\exp\left(-\left\| f_\theta(\boldsymbol{x}) - \boldsymbol{\mu}_c \right\|_2^2\right)}{\sum_{k=1}^{C} \exp\left(-\left\| f_\theta(\boldsymbol{x}) - \boldsymbol{\mu}_k \right\|_2^2\right)} \tag{7}$$

Finally, we can define the *CL* function as:

$$CL\left(\theta, \{\boldsymbol{\mu}_j\}\right) = -\log p(y \mid \boldsymbol{x}) - \sum\nolimits_{c \neq y} \log\left(1 - p(c \mid \boldsymbol{x})\right) \tag{8}$$

The *CL* function can maximize the probability that the signal deep feature sample $f_\theta(\boldsymbol{x})$ matches with $\boldsymbol{\mu}_y$ while minimizing the probability that the signal deep feature sample $f_\theta(\boldsymbol{x})$ matches with $\boldsymbol{\mu}_c(c \neq y)$, thus ensuring classification of the known signal.

For the *DL* function, we first calculate the distance between the signal deep feature $f_\theta(\boldsymbol{x})$ and the corresponding intrinsic feature memorizer parameters $\boldsymbol{\mu}_y$ [43]:

$$d\left(\boldsymbol{x}, \boldsymbol{\mu}_y\right) = \left\| f_\theta(\boldsymbol{x}) - \boldsymbol{\mu}_y \right\|_2^2 \tag{9}$$

We then calculate the distance between the same signal deep feature sample $f_\theta(\boldsymbol{x})$ and the intrinsic feature memorizer parameters $\boldsymbol{\mu}_c(c \neq y)$ that belong to other known signal classes:

$$d\left(\boldsymbol{x}, \boldsymbol{\mu}_c\right) = \left\| f_\theta(\boldsymbol{x}) - \boldsymbol{\mu}_c \right\|_2^2 \tag{10}$$

Finally, we can define the *DL* function as:

$$DL\left(\theta, \{\boldsymbol{\mu}_j\}\right) = d\left(\boldsymbol{x}, \boldsymbol{\mu}_y\right) + \frac{1}{\sum_{c \neq y} d\left(\boldsymbol{x}, \boldsymbol{\mu}_c\right)} \tag{11}$$

The *DL* function can minimize the distance between the signal deep feature sample $f_\theta(\boldsymbol{x})$ and $\boldsymbol{\mu}_y$, while maximizing the distance between the signal deep feature sample $f_\theta(\boldsymbol{x})$ and $\boldsymbol{\mu}_c(c \neq y)$. This allows the signal deep feature sample $f_\theta(\boldsymbol{x})$ to be clustered around $\boldsymbol{\mu}_y$ as much as possible and reduces the possibility of intersection with the deep feature samples of other classes including unknown classes, as shown in **Fig. 2(b)**. Thus, the detection of unknown signal class is achieved.

As such, the loss function of the open-set SEI network can be expressed as

$$L\left(\theta, \{\boldsymbol{\mu}_j\}\right) = CL\left(\theta, \{\boldsymbol{\mu}_j\}\right) + \lambda \cdot DL\left(\theta, \{\boldsymbol{\mu}_j\}\right) \tag{12}$$

where λ represents the regularization weighting coefficient.

The deep feature extractor parameter θ and intrinsic feature memorizer parameter $\{\boldsymbol{\mu}_j\}$ were optimized using a backpropagation algorithm:

$$\theta \leftarrow \theta - \eta_1 \cdot \frac{\partial L\left(\theta, \{\boldsymbol{\mu}_j\}\right)}{\partial \theta} \tag{13}$$

$$\{\boldsymbol{\mu}_j\} \leftarrow \{\boldsymbol{\mu}_j\} - \eta_2 \cdot \frac{\partial L\left(\theta, \{\boldsymbol{\mu}_j\}\right)}{\partial \{\boldsymbol{\mu}_j\}} \tag{14}$$

where η_1 and η_2 are the open-set SEI network learning rates.

After training, a threshold ξ was set to detect unknown signal classes i.e.,

$$\max_{j=1}^{C} d\left(\boldsymbol{x}, \boldsymbol{\mu}_j\right) = \max_{j=1}^{C} \left\| f_\theta\left(\boldsymbol{x}\right) - \boldsymbol{\mu}_j \right\|_2^2 > \xi \tag{15}$$

The testing signal sample $\boldsymbol{x}$ is then detected as an unknown signal class. Otherwise, it is classified as y, which is a known signal class:

$$y = \operatorname*{argmax}_{j=1}^{C} p\left(j \mid \boldsymbol{x}\right) = \operatorname*{argmax}_{j=1}^{C} \frac{\exp\left(-\left\| f_\theta\left(\boldsymbol{x}\right) - \boldsymbol{\mu}_j \right\|_2^2\right)}{\sum_{k=1}^{C} \exp\left(-\left\| f_\theta\left(\boldsymbol{x}\right) - \boldsymbol{\mu}_k \right\|_2^2\right)} \tag{16}$$

3.2 Addressing Open-set SEI with limited samples: A Meta-Learning-based Approach

SEI technology is mainly applied to non-cooperative scenarios, and only a few labeled signal samples can be obtained and used for training. In this regard, a deep-learning-based training algorithm loses its advantage, i.e., the network can only achieve excellent identification performance by relying on large-scale labeled signal samples. To solve the few-shot problem in an open-set SEI, we propose a meta-learning algorithm to train the open-set SEI network.

Meta-learning [44], also known as learning to learn, refers to network learning for many similar tasks by constantly adapting to each specific task so that the network is capable of acquiring abstract knowledge. Unlike general machine learning algorithms, the basic training unit of the meta-learning model is a task, and the dataset used for the training and testing procedures in each task is called the support set and query set, respectively. Within each task, the parameters of the open-set SEI network are assigned to a temporary network, which is then optimized using the support set. The performance of the temporary network is then evaluated based on the query set, and the gradient loss is computed and collected to further optimize the open-set SEI network. Meta-learning has developed into an effective method for solving the few-shot problem because of its capability to address different new tasks based on the meta-knowledge acquired from a few samples. Therefore, the application of a meta-learning approach to the training of open-set SEI networks can effectively address open-set SEI with limited samples.

We collected a training database D_{train} containing the signal representation vectors $\boldsymbol{x}$ with the corresponding class label y and sample M meta-training tasks $T = \left\{T_1, T_2, \cdots, T_n, \cdots, T_M\right\}$ from D_{train}. Assuming that D_{train} contains C_1 classes of signal representation vectors, $C_2\left(C_2 < C_1\right)$ classes of signal representation vectors are randomly selected to construct a sub-training database $D_{sub-train}$, and P samples in each class of C_2 are randomly selected to form a support set $S_i = \left\{\left(\boldsymbol{x}_s^{(i)}, y_s^{(i)}\right)\right\}$ containing $C_2 \times P$ samples. The remaining R samples in each class of C_2 are then selected, and a query set $Q_i = \left\{\left(\boldsymbol{x}_q^{(i)}, y_q^{(i)}\right)\right\}$ containing $C_2 \times R$ samples is constructed. Finally, the support set S_n and query set Q_n are combined to obtain task T_i.

Meta-training and optimization are then performed for the open-set SEI network with different tasks to obtain meta-knowledge. For task T_i, the loss function of the open-set SEI

network in (12) can be calculated using support set $S_i = \left\{\left(\boldsymbol{x}_s^{(i)}, y_s^{(i)}\right)\right\}$, which can be expressed as

$$L_{T_i}\left(\left(\boldsymbol{x}_s^{(i)}, y_s^{(i)}\right); \theta, \left\{\boldsymbol{\mu}_j\right\}\right) = CL_{T_i}\left(\left(\boldsymbol{x}_s^{(i)}, y_s^{(i)}\right); \theta, \left\{\boldsymbol{\mu}_j\right\}\right) + \lambda \cdot DL_{T_i}\left(\left(\boldsymbol{x}_s^{(i)}, y_s^{(i)}\right); \theta, \left\{\boldsymbol{\mu}_j\right\}\right) \quad (17)$$

Based on the result of Equation (17), the temporary network parameters, including the deep feature extractor parameters $\varphi^{(i)}$ and the intrinsic feature memorizer parameters $\left\{\boldsymbol{\mu}_j\right\}^{(i)}$ in task T_i are optimized using the gradient descent method:

$$\varphi^{(i)} = \theta - \alpha \cdot \frac{\partial L_{T_i}\left(\left(\boldsymbol{x}_s^{(i)}, y_s^{(i)}\right); \theta, \left\{\boldsymbol{\mu}_j\right\}\right)}{\partial \theta} \quad (18)$$

$$\left\{\boldsymbol{\mu}_j\right\}^{(i)} = \left\{\boldsymbol{\mu}_j\right\} - \beta \cdot \frac{\partial L_{T_i}\left(\left(\boldsymbol{x}_s^{(i)}, y_s^{(i)}\right); \theta, \left\{\boldsymbol{\mu}_j\right\}\right)}{\partial \left\{\boldsymbol{\mu}_j\right\}} \quad (19)$$

where α and β are temporary network learning rates. we then use the query set $Q_n = \left\{\left(\boldsymbol{x}_q^{(i)}, y_q^{(i)}\right)\right\}$ to calculate the gradient loss of the temporary network:

$$\nabla_{\varphi^{(i)}} = \frac{\partial L_{T_i}\left(\left(\boldsymbol{x}_q^{(i)}, y_q^{(i)}\right); \varphi^{(i)}, \left\{\boldsymbol{\mu}_j\right\}^{(i)}\right)}{\partial \varphi^{(i)}} \quad (20)$$

$$\nabla_{\left\{\boldsymbol{\mu}_j\right\}^{(i)}} = \frac{\partial L_{T_i}\left(\left(\boldsymbol{x}_q^{(i)}, y_q^{(i)}\right); \varphi^{(i)}, \left\{\boldsymbol{\mu}_j\right\}^{(i)}\right)}{\partial \left\{\boldsymbol{\mu}_j\right\}^{(i)}} \quad (21)$$

Finally, the deep feature extractor parameters θ and intrinsic feature memorizer parameters $\left\{\boldsymbol{\mu}_j\right\}$ of the open-set SEI network are optimized according to the backpropagation algorithm:

$$\theta \leftarrow \theta - \alpha' \cdot \nabla_{\varphi^{(i)}} \quad (22)$$

$$\left\{\boldsymbol{\mu}_j\right\} \leftarrow \left\{\boldsymbol{\mu}_j\right\} - \beta' \cdot \nabla_{\left\{\boldsymbol{\mu}_j\right\}^{(i)}} \quad (23)$$

where α' and β' are the open-set SEI network learning rates.

As such, the meta-training procedure for the open-set SEI network is represented in **Fig. 3**.

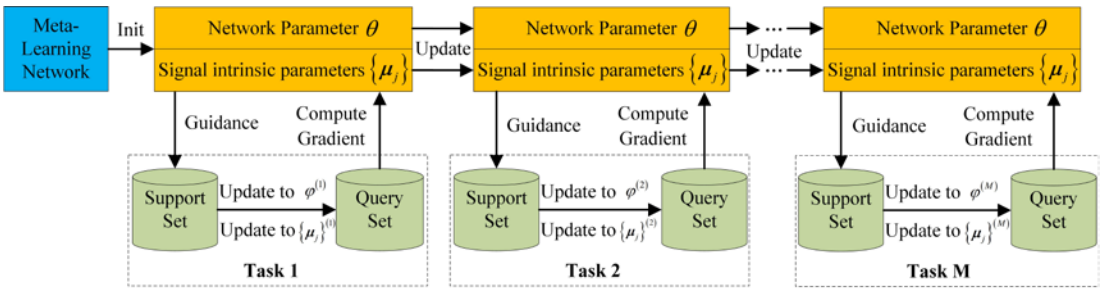

Fig. 3. Meta-training procedure for the open-set SEI network.

As shown in **Fig. 3**, open-set SEI network optimizes its parameters θ and $\{\boldsymbol{\mu}_j\}$ based on the support set $S_i=\left\{\left(\boldsymbol{x}_s^{(i)},y_s^{(i)}\right)\right\}$ within task T_i, thus obtaining the parameters of temporary network $\varphi^{(i)}$ and $\{\boldsymbol{\mu}_j\}^{(i)}$. Then we use the query set $Q_n=\left\{\left(\boldsymbol{x}_q^{(i)},y_q^{(i)}\right)\right\}$ to evaluate the temporary network to collect the gradient loss to update the open-set SEI network. After meta-training on each task, the open-set SEI network is expected to learn the meta-knowledge.

3.3 Algorithm implementation

The steps involved in the proposed algorithm for open-set SEI are summarized in Algorithm 1.

Algorithm 1 The steps of the proposed algorithm for open-set SEI

Require:

Training database D_{train} and testing database D_{test} composed of signal representation vectors $\boldsymbol{x}$ and their corresponding class labels y;

Initialize the deep feature extractor parameters θ and intrinsic feature memorizer parameters $\{\boldsymbol{\mu}_j\}$ for open-set SEI;

Set the threshold ξ for open-set SEI;

Training Procedure:

1: for $i=1:M$ **do**

2: Randomly sample task $T_i=(S_i,Q_i)$ from training database D_{train};

3: **for** T_i **do**

4: Calculate the loss function of open-set SEI network using S_i by Eq (17);

5: Optimize the deep feature extractor parameters $\varphi^{(i)}$ of temporary network by Eq (18);

6: Optimize the intrinsic feature memorizer parameters $\{\boldsymbol{\mu}_j\}^{(i)}$ of temporary network by Eq (19);

7: Calculate the gradient loss $\nabla_{\varphi^{(i)}}$ of the temporary network using Q_i by Eq (20);

8: Calculate the gradient loss $\nabla_{\{\boldsymbol{\mu}_j\}^{(i)}}$ of the temporary network using Q_i by Eq (21);

9: **end**

10: Optimize the parameters θ and $\{\boldsymbol{\mu}_j\}$ of open-set SEI network by Eq (22) and Eq (23);

11: end

Testing Procedure:

1: Detect unknown signal classes by Eq (15);

2: Classify known signal classes by Eq (16);

4. Results and Discussion

4.1 Experimental data collection and network model setup

The experimental RF signal datasets were generated and collected from 20 USRP devices running on a software-defined radio (SDR) platform, which also included a software toolkit

called GNU Radio, and the Linux operating system Ubuntu 18.04. Each transmitter operated at 2.4 GHz, and the sampling frequency of the receiver was set to 16 MHz. The transmitted RF signal was modulated using quadrature phase-shift keying (QPSK) with a bandwidth of 1.2 MHz. The SDR platform built for our experiments is shown in **Fig. 4**.

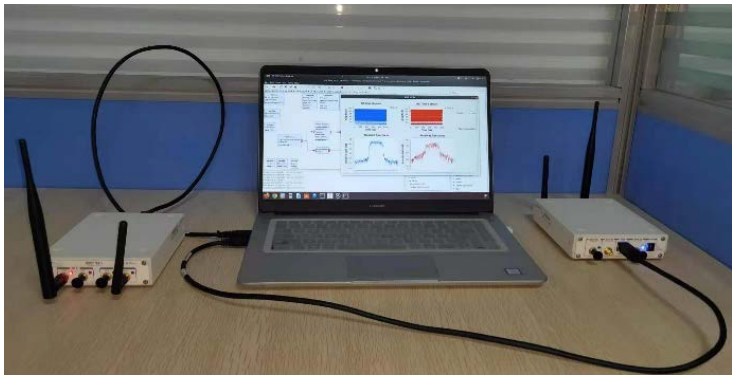

Fig. 4. SDR platform.

To facilitate network model processing, the collected RF signal data were framed, and each frame contained 256 sampling data points. The experimental RF signal datasets were then divided into two parts, each of which contained 10 classes of RF signal data generated by 10 different USRP devices as known and unknown class signal datasets. We sampled 1000 frames of each class of RF signal data from the known part to train the network, then sampled 2000 frames of each class of RF signal data from the known and unknown parts as testing samples to evaluate network performance. Each RF signal data frame was preprocessed using MATLAB 2020a to obtain a signal representation vector, which was used as the input for the open-set SEI network training and testing. The architectural details of the open-set SEI network are shown in **Fig. 5**. The temporary network for meta-learning has the same architectural details as that of the open-set SEI network.

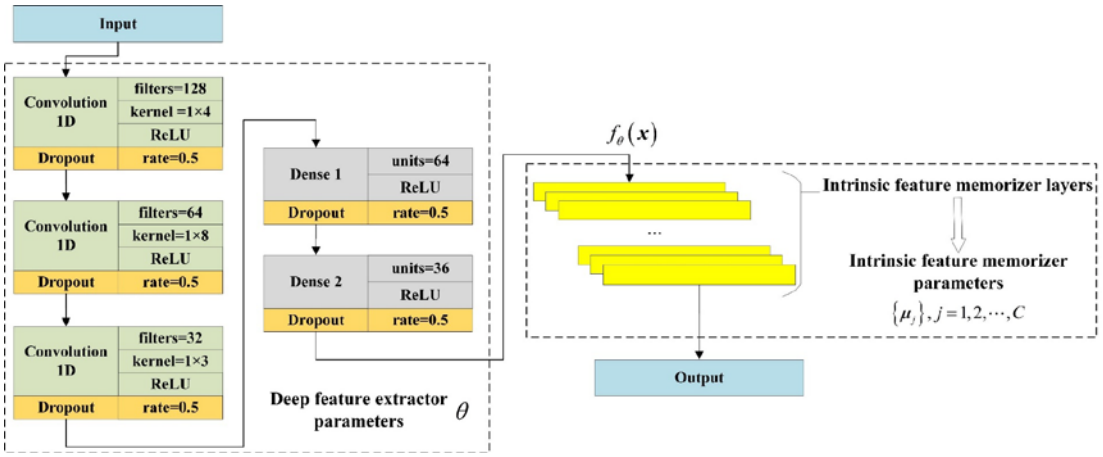

Fig. 5. Architecture details of the open-set SEI network model.

4.2 Open-Set SEI Performance Evaluation

In this section, we evaluate the open-set SEI performance of the proposed method. We set the number of training samples (frames) per class to 1000, then construct a 5-ways 10-shot

task, i.e. 5 of the ten classes of the training RF signals are randomly chosen and 20 training samples (frames) per class are chosen and labeled. In addition, both the support set and the query set of one task contain 5×10 training samples (frames). Finally, 400 meta-learning tasks are generated for meta-learning of the open-set SEI network.

During testing, it is vital to select appropriate evaluation metrics for the open-set SEI performance. It was first necessary to understand the confusion matrix, as shown in **Fig. 6** [22], which is often used to measure the performance of a prediction model on test samples.

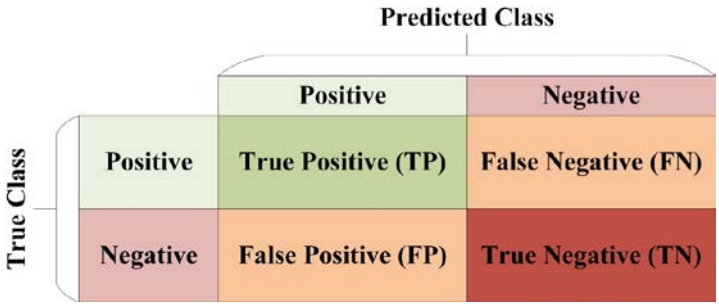

Fig. 6. Confusion matrix of the prediction model.

In general, "accuracy" is the most intuitive evaluation metric for measuring the quality of a classification model. It is the ratio of the samples that are correctly predicted, including true positive (TP) and true negative (TN), to all the samples involved in the prediction, which can be expressed as

$$Accuracy = \frac{TP + TN}{TP + FP + TN + FN} \tag{24}$$

However, accuracy is a global evaluation metric that cannot measure the extent to which a certain class of data is predicted. In this regard, "precision" and "recall" are two alternative evaluation metrics. Precision is the ratio of the positive samples that are correctly predicted to all samples that are predicted to be positive, which can be represented by Eq. (25). Recall is the ratio of the positive samples that are correctly predicted to all available positive samples, which can be represented by Eq. (26).

$$Precision = \frac{TP}{TP + FP} \tag{25}$$

$$Recall = \frac{TP}{TP + FN} \tag{26}$$

To integrate these two evaluation metrics, the F1-score, the harmonic mean of the precision, and recall, were adopted as the final evaluation metrics for open-set SEI performance, which can be expressed as

$$F1-score = \frac{1}{C+1}\sum_{i=1}^{C+1} 2 \times \frac{Precision_i \times Recall_i}{Precision_i + Recall_i} = \frac{1}{C+1}\sum_{i=1}^{C+1} \frac{2TP_i}{2TP_i + FN_i + FP_i} \tag{27}$$

where C denotes the number of known classes, and all unknown classes are defined as belonging to the class $C+1$.

To evaluate the open-set SEI performance, we further introduce the concept of "openness" to describe the degree of the open-set, which can be expressed by Eq. (28):

$$O = 1 - \sqrt{\frac{2 \times C_{TR}}{C_{TR} + C_{TE}}} \tag{28}$$

where C_{TR} and C_{TE} represent the sets of signal classes in the training and testing datasets, respectively. In the experiment, C_{TR} was fixed at 10, which denotes 10 classes of training samples from known class RF signal datasets, and C_{TE} was set to 10, 11, …, 20, which denotes 10 classes of testing samples from known class RF signal datasets and 0, 1, …, 10 classes of testing samples from unknown class RF signal datasets, respectively.

As shown in Eq. (15), a threshold ξ must be set to detect unknown signal classes, which directly affects the open-set SEI performance. In general, if the threshold ξ is set too high, some unknown class samples will be identified as known class samples. In contrast, if the threshold ξ is set too low, some known class samples will be mistakenly detected as unknown class samples. As such, the optimal threshold ξ must be experimentally determined. The threshold ξ is initially set to a value in the range 0–6, with an interval of 0.3. We then collected two, five, eight, and ten classes of testing samples from unknown class RF signal datasets to perform open-set SEI and plot the F1-score versus thresholds, as shown in **Fig. 7**.

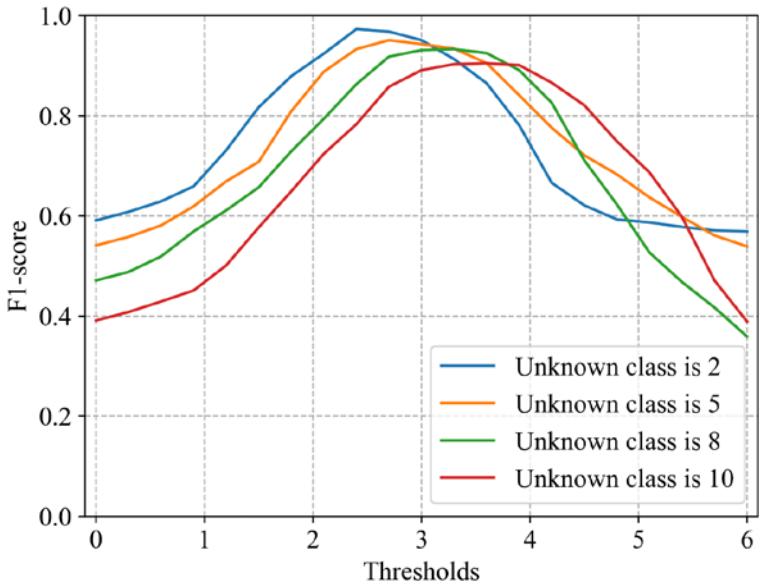

Fig. 7. F1-score vs. thresholds for different numbers of unknown classes.

As shown in **Fig. 7**, there are peaks in all four curves of the F1-score vs. thresholds plots, which confirm the previous analysis. In addition, the distribution of the thresholds ξ corresponding to the peaks of all four curves is concentrated at approximately 3. Therefore, we set the threshold as $\xi = 3$ to optimally perform open-set SEI.

Then, we compared the proposed method with the state-of-the-art methods proposed in [33] and [34] for SEI to highlight the superiority of our approach. Finally, we plot and compare the F1-score versus the "openness" of various methods. The experimental results are shown in **Fig. 8**.

As shown in **Fig. 8**, the F1-score of the three methods were approximately equal and reached almost 100% when the openness value was 0, indicating excellent closed-set SEI performance

of the three methods. As the openness increases, the F1-score of the proposed method and the other two methods decrease to different degrees. However, the presented approach still maintains a high F1-score and the value can reach more than 90% even when the class of unknown open-set RF signals increases to 10. In contrast, the F1-score of the other two methods decrease significantly, and the gap between these techniques and the proposed method gradually increases. When the openness value is a maximum, the gap is 14%–18%. These experimental results were obtained because the network model of the proposed approach can detect and exclude RF signals of unknown classes using an intrinsic feature memorizer, thus avoiding adverse effects during the classification of RF signals of known classes. However, the network model design of the other two state-of-the-art methods is based on closed-set assumptions. RF signals from unknown classes can only be forced to be classified as a specific known class, thus greatly affecting the identification performance, particularly when the openness value increases. Therefore, the effectiveness and superiority of the proposed approach were demonstrated based on the results of comparative experiments.

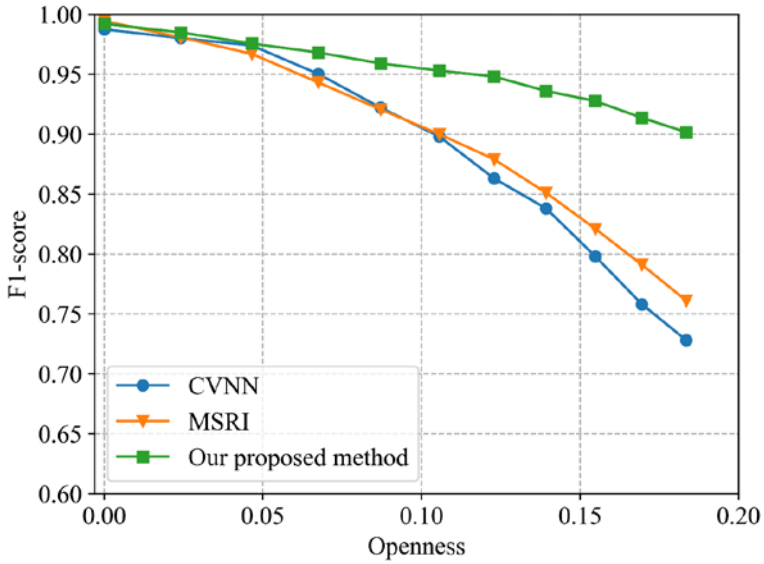

Fig. 8. F1-score vs. openness of various methods.

4.3 Open-set SEI performance vs. Number of training samples

In the experiment described in Section 4.2, the number of training samples was set to 1000, which is a large-scale training set for an open-set SEI. However, in non-cooperative scenarios, only a limited number of training samples are available. Therefore, we proposed a meta-learning-based approach to address the few-shot problem of open-set SEI.

To verify the influence of the number of training samples on the open-set SEI performance, we reduced the number of training samples per class from 800 to 200 at intervals of 200 based on the results in Section 4.2. We then tested and compared the open-set SEI performance of various methods. The experimental results are presented as plots of the F1-score vs. openness, as shown in **Fig. 9**.

As shown in **Fig. 9**, as the number of training samples decreases, the F1-score of the proposed method remains unchanged compared to **Fig. 8**. In contrast, the open-set SEI performance of the other two state-of-the-art methods decreases when there are fewer training samples. In particular, when the number of training samples decreased to 200, the F1-score of the two methods is below 55% when openness has a maximum value, and the difference in

comparison to the proposed method was more than 35%. The experimental results demonstrate the superiority of the presented technique in performing open-set SEI tasks with limited training samples.

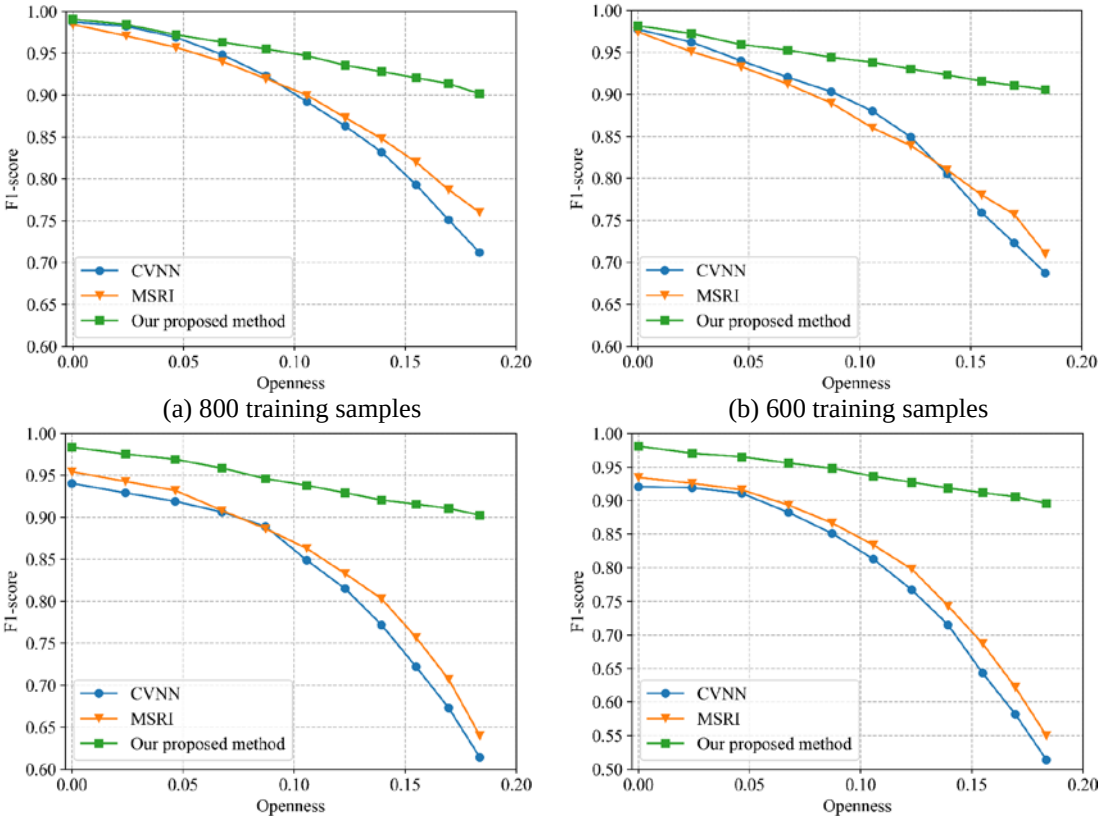

(a) 800 training samples (b) 600 training samples

(c) 400 training samples (d) 200 training samples

Fig. 9. F1-score vs. openness of various methods with different training samples: (a) 800 training samples, (b) 600 training samples, (c) 400 training samples, and (d) 200 training samples.

To explore the potential of the proposed method in dealing with a few-shot open-set SEI, we further reduced the number of training samples per class from 150 to 50 in steps of 50, and evaluated the open-set SEI performance. The experimental results are presented as plots of the F1-score vs. openness, as shown in **Fig. 10**.

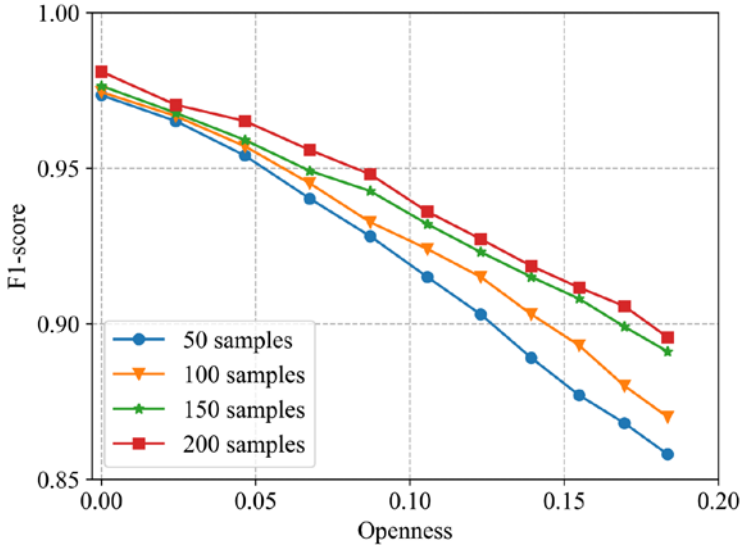

Fig. 10. F1-score vs. openness of the proposed method for 200, 150, 100, and 50 training samples.

The experimental results indicate that, as the number of training samples decreases, the F1-score of the proposed method begins to decline, but not significantly. As shown in **Fig. 10**, when the number of training samples is reduced to a minimum of 50, the proposed approach achieved a relatively high F1-score of more than 85% for the maximum value of openness. In conclusion, the proposed method is effective for addressing the few-shot problem of open-set SEI.

4.4 Visualization analysis

To more intuitively observe the open-set SEI capability of the proposed method, we use the t-distributed stochastic neighbor embedding (t-SNE) [45] algorithm to achieve dimensionality reduction to show deep signal features.

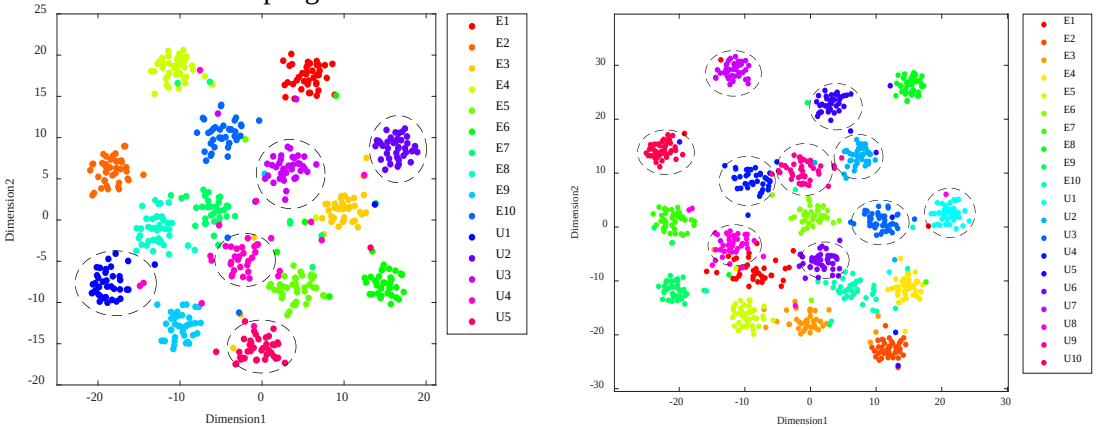

(a) Five unknown classes of RF signals (b) Ten unknown classes of RF signals

Fig. 11. Two-dimensional scatterplot of signal deep features after dimensionality reduction: (a) 5 unknown classes of RF signals; (b) 10 unknown classes of RF signals.

During the visualization experiments, 10 known classes of RF signals and 5 (10) unknown classes of RF signals were utilized for open-set SEI network processing, and the penultimate

layer output vector $f_\theta(\boldsymbol{x})$, also called the signal deep features, was dimensionally reduced using the t-SNE algorithm to a two-dimensional scatterplot, as shown in **Fig. 11**.

As shown in **Fig. 11**, E1–E10 represents the 10 known classes of RF signals, and U1–U5 (U10) represents the 5 (10) unknown classes of RF signals, for which the corresponding two-dimensional scattered points all form clusters. All clusters of known classes showed high aggregation and there are distinct boundaries between different clusters. In addition, the clusters of unknown classes, highlighted using dashed lines, also have less overlap with the clusters of known classes. This is because of the introduction of an intrinsic feature memorizer that can optimize the network training process, so that the open-set SEI network can extract signal deep features with good intra-class aggregation and inter-class differentiation. As a result, the system can effectively distinguish between the RF signals of known and unknown classes and efficiently classify the RF signals of known classes. In conclusion, the results of the visualization analysis experiments provide additional evidence of the excellent open-set SEI performance of the proposed method from the perspective of RF signal deep-feature extraction.

4.5 Noise robustness

The aforementioned experimental results demonstrate the effectiveness and superiority of the proposed method. However, the signal data were obtained in a laboratory environment, and the SNR exceeded 50 dB in preliminary measurements. Thus, noise pollution was not a factor. However, noise interference is inevitable in the practical application of this technology. Therefore, noise robustness is a crucial aspect in evaluating the performance of the proposed method.

In this section, we used MATLAB to introduce additive white Gaussian noise (AWGN) to the acquired experimental signal dataset such that the SNR was -20, -18,..., 18, and 20 dB. We then sampled 50, 100, 150, and 200 samples per class of RF signal for network training. During testing, we utilized 10 known classes of RF signals and 2, 5, 8, and 10 unknown classes of RF signals to evaluate the noise robustness of the proposed method.

As shown in **Fig. 12**, at each SNR, it is possible to achieve almost the same F1-score using different numbers of training samples, which increases with an increase in the SNR. As shown in **Fig. 12(a)** and **Fig. 12(b)**, when there are two and five unknown classes of RF signals, respectively, the F1-score exceeds 90% when the SNR has values of 8 dB and 10 dB, respectively, and remains stable for higher SNR values. Furthermore, when the unknown classes of RF signals increase to eight and ten classes, the F1-score exceeds 85% when the SNR is 10 dB, and remains stable for higher SNR values, as shown in **Fig. 12(c)** and **Fig. 12(d)**. The experimental results show that not only can the proposed method adapt to the open-set SEI with limited training samples in the presence of noise interference, but it can also achieve and maintain high open-set SEI performance at low SNRs, which is indicative of strong anti-noise performance and excellent noise robustness.

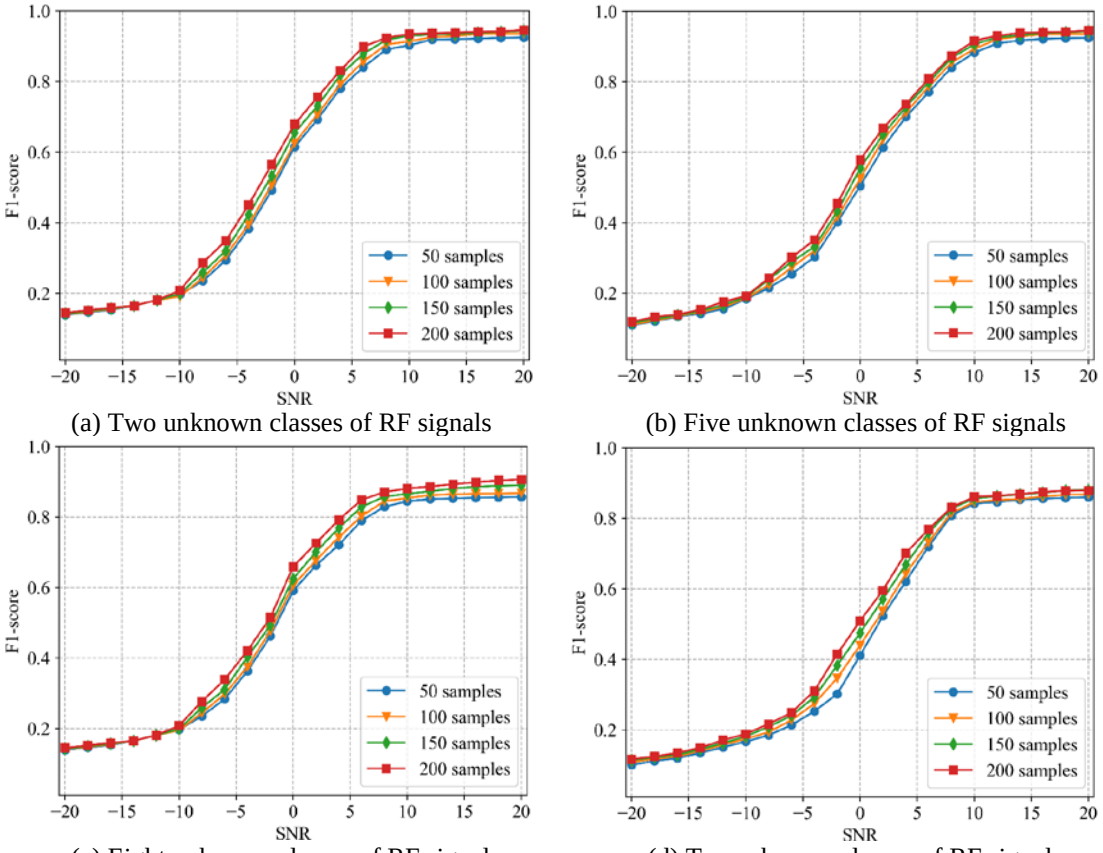

(a) Two unknown classes of RF signals (b) Five unknown classes of RF signals

(c) Eight unknown classes of RF signals (d) Ten unknown classes of RF signals

Fig. 12. F1-score vs. SNR for the proposed method with different numbers of unknown classes: (a) two unknown classes of RF signals, (b) five unknown classes of RF signals, (c) eight unknown classes of RF signals, and (d) ten unknown classes of RF signals.

5. Conclusion

A meta-learning-based open-set identification system for SEI in non-cooperative scenarios is proposed. We developed a signal preprocessing scheme based on bi-spectral analysis and the Radon transform to highlight the discriminability of individual emitters. An open-set SEI network was then proposed, which consisted of a deep feature extractor and an intrinsic feature memorizer, and the training loss functions and procedure for the open-set SEI network are described. To solve the few-shot problem of the open-set SEI, we further designed a meta-training loss function and meta-training procedure based on the original open-set SEI network. The experimental results indicate that the proposed method can successfully detect the presence of RF signals in unknown classes and effectively distinguish among known classes of RF signals. Moreover, the proposed method had a higher open-set SEI performance compared to the state-of-the-art methods. Its superiority was apparent based on the improvement in the degree of openness and the reduction of the number of training samples. In addition, the proposed approach exhibited strong noise robustness, and its open-set SEI performance was maintained at a high level at low SNRs. In summary, the proposed method can be adapted to SEI tasks in non-cooperative scenarios.

Acknowledgement

This work was supported in part by the National Natural Science Foundation of China under Grant 91538201, in part by Taishan Scholar Project of Shandong Province under Grant ts201511020, and in part by Project supported by Chinese National Key Laboratory of Science and Technology on Information System Security under Grant 6142111190404.

References

[1] M. Li, O. Li, G. Liu, C. Zhang, "Generative adversarial networks-based semi-supervised automatic modulation recognition for cognitive radio networks," *Sensors*, vol. 18, no. 11, pp. 1–22, 2018. Article(CrossRef Link)

[2] G. Kakkavas, K. Tsitseklis, V. Karyotis and S. Papavassiliou, "A software defined radio cross-layer resource allocation approach for cognitive radio networks: from theory to practice," *IEEE Transactions on Cognitive Communications and Networking*, vol. 6, no. 2, pp. 740-755, 2020. Article(CrossRef Link)

[3] T. -Y. Xiong, Y. -D. Yao, Y. -J. Ren, Z. Li, "Multiband spectrum sensing in cognitive radio networks with secondary user hardware limitation: random and adaptive spectrum sensing strategies," *IEEE Transactions on Wireless Communications*, vol. 17, no. 5, pp. 3018–3029, 2018. Article(CrossRef Link)

[4] X. Liu, C. Sun, M. Zhou, C. Wu, B. Peng and P. Li, "Reinforcement learning-based multislot double-threshold spectrum sensing with bayesian fusion for industrial big spectrum data," *IEEE Transactions on Industrial Informatics*, vol. 17, no. 5, pp. 3391-3400, 2021. Article(CrossRef Link)

[5] S. Haykin, "Cognitive radio: Brain-empowered wireless communications," *IEEE Journal on Selected Areas in Communications*, vol. 23, no. 2, pp. 201–220, 2005. Article(CrossRef Link)

[6] A. Ghosh, W. Hamouda, "Cross-layer antenna selection and channel allocation for MIMO cognitive radios," *IEEE Transactions on Wireless Communications*, vol. 10, no. 11, pp. 3666–3674, 2011. Article(CrossRef Link)

[7] V. Shakhov I. Koo, "Analysis of a network stability-aware clustering protocol for cognitive radio sensor networks," *IEEE Internet of Things Journal*, vol. 8, no. 15, pp. 12476-12477, 2021. Article(CrossRef Link)

[8] Y. Pei, Y.-C. Liang, K. C. Teh, K. -H. Li, "How much time is needed for qideband spectrum sensing?," *IEEE Transactions on Wireless Communications*, vol. 8, no. 11, pp. 5466–5471, 2009. Article(CrossRef Link)

[9] J. Sheng, F.-L. Liu, Z. -X. Zhang, C. -M. Huang, "TCVQ-SVM algorithm for narrowband spectrum sensing," *Physical Communication*, vol. 50, no. 11, 2022, article ID 101502. Article(CrossRef Link)

[10] X. -L. Wang, Y.-B. Ji, H. -X. Zhang, et al, "Radio frequency signal identification using transfer learning based on LSTM," *Circuits, Systems, and Signal Processing*, vol. 39, pp. 5514–5528, 2020. Article(CrossRef Link)

[11] J. Han, T. Zhang, Z.-Y. Qiu, X.-Y. Zheng, "Communication emitter individual identification via 3D−Hilbert energy spectrum−based multiscale segmentation features," *Communication systems*, vol. 32, no. 1, pp. 1–13, 2018. Article(CrossRef Link)

[12] K. Merchant, S. Revay, G. Stantchev and B. Nousain, "Deep learning for RF device fingerprinting in cognitive communication networks," *IEEE Journal of Selected Topics in Signal Processing*, vol. 12, no. 1, pp. 160–167, 2018. Article(CrossRef Link)

[13] A.E. Spezio, "Electronic warfare systems," *IEEE Transactions on Microwave Theory and Techniques*, vol. 50, no. 3, pp. 633–644, 2002. Article(CrossRef Link)

[14] X. Tian, X. Wu, H. Li and X. Wang, "RF fingerprints prediction for cellular network positioning: A subspace identification approach," *IEEE Transactions on Mobile Computing*, vol. 19, no. 2, pp. 450-465, 2020. Article(CrossRef Link)

[15] S. Rajendran, Z. Sun, F. Lin and K. Ren, "Injecting reliable radio frequency fingerprints using metasurface for the internet of things," *IEEE Transactions on Information Forensics and Security*, vol. 16, pp. 1896-1911, 2020. Article(CrossRef Link)
[16] P. Padilla, J.L. Padilla, and J.F. Valenzuela-Valdés, "Radiofrequency identification of wireless devices based on RF fingerprinting," *Electronics Letters*, vol. 49, no. 22, pp. 1409–1410, 2013. Article(CrossRef Link)
[17] Y. -J. Yuan, Z. -T. Huang, H. Wu, X. Wang, "Specific emitter identification based on Hilbert–Huang transform-based time–frequency–energy distribution features," *IET Communications*, vol. 8, pp. 2404–2412, 2014. Article(CrossRef Link)
[18] U. Satija, N. Trivedi, G. Biswal, B. Ramkumar, "Specific emitter identification based on variational mode decomposition and spectral features in single hop and relaying scenarios," *IEEE Transactions on Information Forensics and Security*, vol. 14, no. 3, pp. 581–591, 2019. Article(CrossRef Link)
[19] Y. -P. Zhou, X. Wang, Y. Chen, Y. Tian, "Specific emitter identification via bispectrum-radon transform and hybrid deep model," *Mathematical Problems Engineering*, 2020, 17 pages article ID 7646527. Article(CrossRef Link)
[20] S. Vimal, R. Y. Harold, M. Kaliappan, et al, "AI based forecasting of influenza patterns from twitter information using random forest algorithm," *Human-centric Computing and Information Sciences*, vol. 11, no. 33, pp. 1–15, 2021. Article(CrossRef Link)
[21] D. Murat, B. Catherine, "The effects of domain knowledge on trust in explainable AI and task performance: A case of peer-to-peer lending," *International Journal of Human-Computer Studies*, vol. 162, 2022, article ID 102792. Article(CrossRef Link)
[22] H. Mohamed, M. I. Abdullah, A. E. Ibrahim, et al, "End-to-end data authentication deep learning model for securing IoT configurations," *Human-centric Computing and Information Sciences*, vol. 12, no. 4, pp. 1–19, 2022. Article(CrossRef Link)
[23] J. -W. Su, B. -Y. Xu, H. J. Yin, "A survey of deep learning approaches to image restoration," *Neurocomputing*, vol. 487, pp. 46–65, 2022. Article(CrossRef Link)
[24] Y. Lin, Y. Tu and Z. Dou, "An improved neural network pruning technology for automatic modulation classification in edge devices," *IEEE Transactions on Vehicular Technology*, Vol. 69, no. 5, pp. 5703-5706, 2020. Article(CrossRef Link)
[25] X. Zhang et al., "NAS-AMR: neural architecture search based automatic modulation recognition for integrated sensing and communication systems," *IEEE Transactions on Cognitive Communications and Networking*, 2022. Article(CrossRef Link)
[26] Y. Lin, Y. Tu, Z. Dou, L. Chen and S. Mao, "Contour Stella Image and Deep Learning for Signal Recognition in the Physical Layer," *IEEE Transactions on Cognitive Communications and Networking*, vol. 7, no. 1, pp. 34-46, 2021. Article(CrossRef Link)
[27] Y. Tu et al., "Large-scale real-world radio signal recognition with deep learning," *Chinese Journal of Aeronautics*, 2021. Article(CrossRef Link)
[28] L. Ding, S. -L. Wang, F. -G. Wang, et al., "Specific emitter identification via convolutional neural networks," *IEEE Communications Letters*, Vol. 22, no. 12, pp. 2591-2594, 2018. Article(CrossRef Link)
[29] Y. -W. Pan, S. -H. Yang, H. Peng, et al., "Specific emitter identification based on deep residual networks," *IEEE Access*, vol. 7, pp. 54425-54434, 2019. Article(CrossRef Link)
[30] G. Baldini, C. Gentile, R. Giuliani, et al., "Comparison of techniques for radiometric identification based on deep convolutional neural networks," *Electronics Letters*, vol. 55, no. 2, pp. 90-92, 2019. Article(CrossRef Link)
[31] L. -J. Wong, W. C. Headley, and A. J. Michaels, "Specific emitter identification using convolutional neural network-based IQ imbalance estimators," *IEEE Access*, vol. 7, pp. 33544-33555, 2019. Article(CrossRef Link)
[32] Y. -G. Liu, H. Xu, Z. -S. Qi, and Y. Shi, "Specific emitter identification against unreliable features interference based on time-series classification network structure," *IEEE Access*, vol. 8, pp. 200194–200208, 2020. Article(CrossRef Link)

[33] Y. Wang, G. Gui, H. Gacanin, et al, "An efficient specific emitter identification method based on complex-valued neural networks and network compression," *IEEE Journal on Selected Areas in Communications*, vol. 39, pp. 2305–2317, 2021. Article(CrossRef Link)
[34] Y. -H. Qian, J. Qi, X. -Y. Kuai, et al, "Specific emitter identification based on multi-level sparse representation in automatic identification system," *IEEE Transactions on Information Forensics and Security*, vol. 16, pp. 2872–2884, 2021. Article(CrossRef Link)
[35] Z. Sun, S. Kong and W. Wang, "Sparse learning of higher-order statistics for communications and sensing," *IEEE Transactions on Emerging Topics in Computational Intelligence*, vol. 4, no. 1, pp. 13–22, 2020. Article(CrossRef Link)
[36] L. -H. Zhang, Y. Wang, D. -W. Zhang, "Research on multiple-image encryption mechanism based on Radon transform and ghost imaging," *Optics Communications*, vol. 504, 2022, article ID 127494. Article(CrossRef Link)
[37] A. Gholami, M. Farshad, "Fast hyperbolic Radon transform using chirp-z transform," *Digital Signal Processing*, vol. 87, pp. 34–42, 2019. Article(CrossRef Link)
[38] Y. -F. Peng, S. -W. Tian, L. Yu, et al, "Malicious URL recognition and detection using attention-based CNN-LSTM," *KSII Transactions on Internet and Information Systems*, vol. 13, no. 11, pp. 5580-5593, 2019. Article(CrossRef Link)
[39] G. Choe, S. Lee and J. Nang, "CNN-based visual/auditory feature fusion method with frame selection for classifying video events," *KSII Transactions on Internet and Information Systems*, vol. 13, no. 3, pp. 1689-1701, 2019. Article(CrossRef Link)
[40] W. J. Scheirer, A. de Rezende Rocha, A. Sapkota, T. E. Boult, "Toward open set recognition," *IEEE Transactions on Pattern Analysis and Machine Intelligence*, vol. 35 pp. 1757–1772, 2013. Article(CrossRef Link)
[41] W. J. Scheirer, L. P. Jain, and T. E. Boult, "Probability models for open set recognition," *IEEE Transactions on Pattern Analysis and Machine Intelligence*, vol. 36 pp. 2317–2324, 2014. Article(CrossRef Link)
[42] B. Abhijit and E.B. Terrance, "Towards open set deep networks," in *Proc. of IEEE Conference on Computer Vision and Pattern Recognition*, Las Vegas, USA, pp. 1563–1572, 2016. Article(CrossRef Link)
[43] Y. Wen, K. Zhang, Z. Li, and Q. Yu, "A discriminative feature learning approach for deep face recognition," in *Proc. of European Conference on Computer Vision*, Amsterdam, Netherlands, 499–515, 2016. Article(CrossRef Link)
[44] T. -Y. Mu, H. -Z. Wang, C. -N. Wang, et al, "Auto-CASH: A meta-learning embedding approach for autonomous classification algorithm selection," *Information Sciences*, vol. 591, pp. 344-364, 2022. Article(CrossRef Link)
[45] A. Gisbrecht, A. Schulz, B. Hammer, "Parametric nonlinear dimensionality reduction using kernel t-SNE," *Neurocomputing*, vol. 147, pp. 71–82, 2015. Article(CrossRef Link)

CUNXIANG XIE was born in Yantai, Shandong, China, in 1996. He received the B.S. degree in communication engineering from the Naval Aviation University, in 2019. He is currently pursuing the M.S. degree in information and communication engineering with the Department of Information Fusion, Naval Aviation University. His research interests include deep learning and specific emitter identification.

LIMIN ZHANG was born in Kaiyuan, Liaoning, China, in 1966. He received the Ph.D. degree in signal processing technology from the Tianjin University, in 2005. Since 2005, he has been a Professor with the Naval Aviation University. His research interests include satellite communication signal processing.

ZHAOGEN ZHONG was born in Nanchang, Jiangxi, China, in 1984. He received the Ph.D. degree in information and communication engineering from the Naval Aviation University, in 2013. He is currently an Associate Professor with the Naval Aviation University. His research interests include spread spectrum signal processing.